sciendo

POLISH MARITIME RESEARCH 1 (121) 2024 Vol. 31; pp. 16-23
10.2478/pomr-2024-0002

ANALYTICAL AND EXPERIMENTAL INVESTIGATION OF ASYMMETRIC FLOATING PHENOMENA OF UNIFORM BODIES

Jian Gu [1,2] *
Antonio Carlos Fernandes [3]
Wei Chai [4]
Shu Xia Bu [1,2]
Xiangxi Han [5]
[1.] China Ship Scientific Research Center, China
[2.] Taihu Laboratory of Deepsea Technological Science, China
[3] Federal University of Rio de Janeiro , Brazil
[4] Wuhan University of Technology, China
[5] Beibu Gulf University, China

* Corresponding author: *joson_gu@yahoo.com (Jian Gu)*

ABSTRACT

Uniform symmetric bodies can be observed floating asymmetrically under certain circumstances. Previous explanations of this are mostly abstract and lack experimental verification, making their understanding and application difficult. This article presents in detail alternative insights into the floating equilibria of uniform prisms and parabolic cylinders. The intrinsic characteristics of the equilibrium curves are investigated, and several equilibria different from those in the literature are found. The inflection points in the equilibrium curves are analyzed quantitatively due to their significance for floating states. Furthermore, experiments have been conducted for the square prism which validate the derived equilibrium curve, and provide a practical impression of the asymmetric floating phenomenon of symmetric bodies. These results have the potential to be applied in naval and ocean engineering, such as in the design of vessels and floating offshore structures.

Keywords: hydrostatic stability, floating equilibrium, asymmetric floating state, experimental validation

INTRODUCTION

The stability of floating bodies is a classic and fundamental subject in fluid mechanics. The study of the hydrostatic responses of floating bodies is much earlier than the study of the hydrodynamic response due to the interaction between waves and the floating body[1]. Indeed, it can be traced back to the well-known work of Archimedes[2]. Since then, the interest of researchers and engineers in this subject have never ceased[3][4][5][6]. In naval and ocean engineering, the concept of a meta-centre (denoted by M)[7][8][9][10] has been introduced to evaluate the initial stability of a floating body. It is defined as the intersection of two vertical axes passing through the center of buoyancy at two slightly different angles of heel. What is more, a well-known formulation has been derived, formulating the distance between the buoyancy centre and the meta-centre with the ratio of the moment of inertia of the plane of flotation and the volume of the displaced fluid ($BM = I/\nabla$). A general criterion for the stability of a ship is commonly applied with the use of the meta-center, i.e., the ship remains stable provided the weight and the buoyancy create an upright moment after a limited inclination. Capsizing could happen if the sign of the moment is the opposite. Generally, the meta-centre is assumed consistent at a limited inclination angle ($< 8°$)[11], in the scope of initial stability. Since the ship's hull is usually symmetric, the arm of the upright moment is dependent on the relative position of the meta-centre with respect to the centre of gravity (denoted by G)[12]. The floating state can be regarded as stable, neutral, or unstable when M is located above, on, or below G, respectively. In the preliminary phase of ship design, the stability curve is usually

used to characterize the capability of the hull's maintaining an upright floating state when subjected to limited inclinations. Therefore, the evaluation of the floating equilibrium would be significant for the design of floating structures, especially those involving large variations of weight. To simplify the problem, the present article will start with fundamental homogenous floating bodies.

Physically speaking, could a uniform and symmetric body float asymmetrically in still water? As the general criterion of hydrostatic stability of a floating body is commonly identified under a specified floating state, researchers have attempted to figure out the 'equilibrium' of a random floating state of some fundamental geometries such as a floating ball, circular cylinder, rectangular box, and so on. For example, Auerbach[13]demonstrated that a non-circular cylinder could float indifferently with respect to the cylinder's centra axis. Likewise, Ulam[14]raised a question: whether a uniform body that is able to float stably at any orientation must be a sphere. Assuming the body's density ρ approaches zero, the problem is equivalent to whether a body's being able to hold on in any inclination on a horizontal plane is necessarily a sphere. As a partial answer, Montejano[15]proved that if a body with the above-mentioned character was connected, closed, and bounded, then its shell should be a sphere. This implies that the sphere is one possible geometry with the desired property. Consequently, Gilbert[1] analysed the stable floating equilibrium for several geometries such as an ellipsoid, cylinder and cube, employing the law of minimum energy which is further extended into more complex geometries by Mégel[2]. More recently, a comprehensive review of the floating equilibria of regular solids has contributed to integrating the main results and predicting the potential for applications in engineering[5]. According to the above-mentioned research, a symmetric body is proven theoretically to be able to float asymmetrically. However, the proofs of equilibria are quite abstract, and an extensive investigation of the equilibrium curve is still needed. Also, the characteristics of an equilibrium are yet to be verified by physical experiment.

In naval and ocean engineering, the ship and offshore structures are commonly designed to float in an upright state[3] [4][6]. Meanwhile, the consideration of the entire floating states is practical and crucial under certain circumstances such as improper loading and damage. In the present article, the entire equilibrium curve of stability is, for the uniform square prism and rectangular prism, derived in a more straightforward manner (these are similar to common geometries of a ship hull and of offshore structures like breakwaters and floating piers). Further, the characteristics of the equilibrium curves of a parabolic cylinder with arbitrary profile are extended. With respect to the previous results provided by Gilbert[1], several different characteristics of the equilibrium curve are observed and explained in terms of physics. Furthermore, the floating state of a uniform square prism has been investigated by experiments which validate the theoretical results and provide an experimental impression of the interesting phenomenon that a symmetric floating geometry could float asymmetrically in certain conditions. The present work could be regarded as a preliminary for an extensive study of the floating stability of various more complex floating structures, and demonstrates the asymmetric floating state could be induced by improper loading and design of a floating body with a symmetric sectional profile.

MATHEMATIC MODELLING OF FLOATING EQUILIBRIUM

As shown in Fig. 1, the floating state of a uniform square prism can be represented by its transversal section under the assumption of its being a uniform body. According to Archimedes' principle, the ratio of the draught T to the depth D equals the ratio of the body's density ρ to the density ρ_w of the water, which is denoted by λ ($\lambda = T/D = \rho/\rho_w$). To identify the waterline, a vector $\boldsymbol{n_0}$ is defined normal to the original waterline (blueline) and oriented into the air. Then, the vector can be formulated as $\boldsymbol{n}(-\sin\theta, \cos\theta)$ where θ denotes the angle of inclination relative to the upright state. Setting the origin $O(0,0)$ fixed on the centroid of the immersed edge, the coordinate of the centre of gravity $G(0, D/2)$ and buoyancy $B_0(0, T/2)$ can be formulated at the upright state. Also, any arbitrary centre of buoyancy $B(B_y, B_z)$ can be formulated as a function of λ and θ. It should be noted that the meta-centre M will move along with B until an equilibrium is reached.

The floating states can be classified into two categories according to the geometry of the submerged volume, namely the quadrilateral prism (state 1) or triangular prism (state 2 which includes the critical state). A critical state can be recognized between the states 1 and 2, corresponding to a triangular prism of replacement volume. The floating angle of the critical state can be formulated as $\theta_c = \tan^{-1}(2\lambda)$. To reach a stable floating equilibrium, both the force balance and stability condition should be satisfied, namely $\overrightarrow{BG}//\boldsymbol{n}$ and the vertical coordinate $M_z > G_z$. Thus, the possible floating equilibria can be sought through the variation of λ and θ. Since the floating state is symmetric, the observed range can be reduced to $\lambda \in (0, 1/2]$ and $\theta \in [0, \pi/4]$.

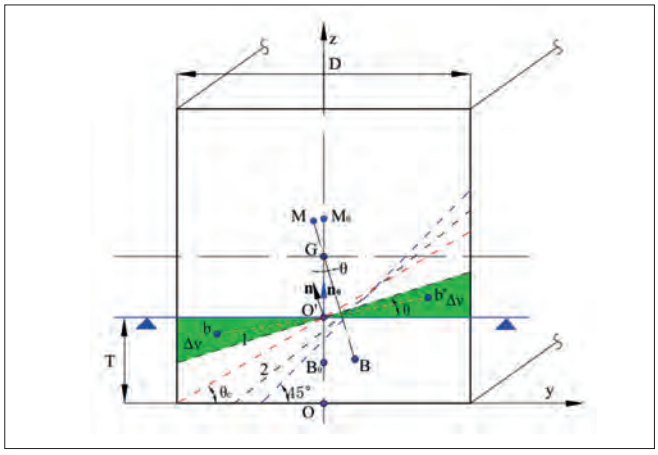

Fig. 1. Illustration of a floating square prism: the green area indicates the equivalent displaced volume of water due to the tilted angle θ; the dashed lines refer to different cases of floating states (in anti-clockwise order: state 1⟶critical state θ_c⟶state 2⟶π/4).

At state 1, i.e., $\theta \in [0, \theta_c)$, the following formulation can be obtained according to Archimedes' principle and the law of the translation of the centre of gravity:

$$(\boldsymbol{B} - \boldsymbol{B_0})V = \Delta \boldsymbol{b} \Delta v \tag{1}$$

where $\boldsymbol{B_0}$ and $\boldsymbol{B}$ refer to the two-dimensional coordinates of the buoyancy centre in the upright and inclined states, respectively. As shown in Fig. 1, $\boldsymbol{b}$ indicates the centre of equivalently translated volume Δv with respect to the total submerged volume V. Substituting the force balance condition $\overrightarrow{BG} // \boldsymbol{n}$ into Eq. (1), one obtains

$$\theta = \cos^{-1}\left(\frac{1}{\sqrt{12\lambda(1-\lambda)-1}}\right) \tag{2}$$

which is valid in the domain $\lambda \in [\frac{3-\sqrt{3}}{6}, 1/2]$. Assuming the condition $\theta < \theta_c$ ($\theta_c = \tan^{-1}(2\lambda)$), the domain can be further reduced to $\lambda \in [\frac{3-\sqrt{3}}{6}, 1/4]$. Accordingly, the stable equilibrium $\theta = 0$ can be obtained in the domain $\lambda \in (0, (3-\sqrt{3})/6)$.

At state 2, the immersed section becomes a triangle in the domain $\theta \in [\theta_c, \pi/4]$. It should be noted that the point $\boldsymbol{O'}$ is not the rotating axis of the flotation plane in this case. Thus, the method of equivalent volume displacement is not available in this case. Employing to the condition $\overrightarrow{BG} // \boldsymbol{n}$, one obtains

$$\theta = \frac{1}{2}\sin^{-1}\left(\frac{16\lambda}{9-16\lambda}\right) \tag{3}$$

which is valid in the domain $\lambda \in [0, 9/32]$. Assuming $\theta \geq \theta_c = \tan^{-1}(2\lambda)$, the domain can be reduced to $\lambda \in [1/4, 9/32]$. Analogously, the equilibrium $\theta = \pi/4$ can be derived in the domain $\lambda \in [9/32, 1/2]$.

In conclusion, the following formula is derived as a function of the angle of inclination θ and the draught ratio λ:

$$\theta = \begin{cases} 0, & \lambda \in (0, \frac{3-\sqrt{3}}{6}] \\ \cos^{-1}\left(\frac{1}{\sqrt{12\lambda(1-\lambda)-1}}\right), & \lambda \in (\frac{3-\sqrt{3}}{6}, \frac{1}{4}] \\ \frac{1}{2}\sin^{-1}\left(\frac{16\lambda}{9-16\lambda}\right), & \lambda \in (\frac{1}{4}, \frac{9}{32}] \\ \pi/4, & \lambda \in (\frac{9}{32}, \frac{1}{2}] \end{cases} \tag{4}$$

As shown in Fig. 2, the stable equilibrium angle θ versus λ is plotted. Notably, there are three inflection points (A, B and C) on the equilibrium curve in the domain $\lambda \in [0, 1/2]$. Observing the curve, one can see the discontinuity at points A and C, which implies severe change of floating state across these points. Comparing this curve with the curve obtained by Gilbert[1], the present curve coincides with it before the inflection point B, but behaves differently approaching to the peak angle, yielding two extra inflections points (B and C).

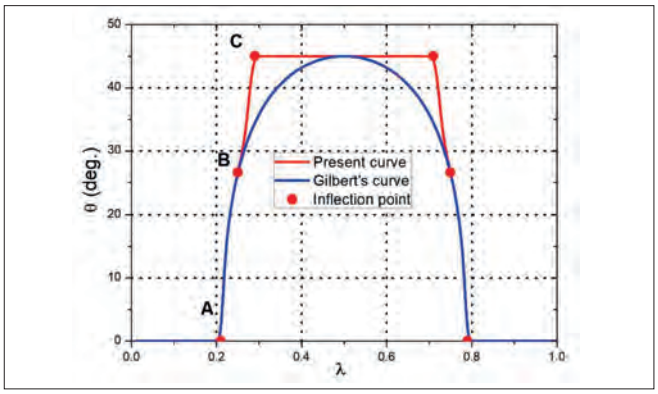

Fig. 2. The comparison of the present equilibrium curve with that of Gilbert [1].

Further, to analyse the implication of the inflection point A, equation (2) can be expressed as

$$\theta = \cos^{-1}(x) \tag{5}$$

where $x = \sqrt{12\lambda(1-\lambda)-1}$. Taking the derivative of λ, equation (5) can be rewritten as

$$\frac{d\theta}{d\lambda} = \frac{6x^2(1-2\lambda)}{\sqrt{1-x^2}} \tag{6}$$

According to equation (5), one can see that x approaches 1 and θ approaches zero when λ approaches $(3 \pm \sqrt{3})/6$. From equation (6), one can see the derivative will approach infinity when x approaches 1, which means it is a singularity and the slope approaches $\pi/2$ at point A.

Similarly, for the inflection point C, equation (3) can be rewritten as

$$\theta = \frac{1}{2}\sin^{-1}(x) \tag{7}$$

where $x = 16\lambda/(9-16\lambda)$. Taking the derivative of λ, equation (7) yields

$$\frac{d\theta}{d\lambda} = \frac{72}{\sqrt{1-x^2}(9-16\lambda)^2} \tag{8}$$

so, analogously, one can find that the derivative will approach infinity as θ approaches $\pi/4$, which implies there is also a singularity whose slope approaches $\pi/2$ at point C. As a result, θ varies severely when λ approaches these singularities.

Meanwhile, the inflection point B is associated to a transitional floating state between states 1 and 2, corresponding to the critical stable equilibrium $\theta = \theta_c$. Combining equation (6) and equation (8), the identical real derivative ($d\theta/d\lambda = 4.8$) can be obtained approaching from both the increasing and decreasing direction. This implies the floating state varies continuously across the inflection point.

PRISM WITH ARBITRARY RECTANGULAR SECTION

The equilibrium curve of a prism with arbitrary rectangulare section can be explored extensively. As shown in Fig. 3, the section of the prism has breadth D and width W (we assume $W > D$). Therefore, the prism will tend to float on the larger

face to be at the minimum of potential energy [1]. Likewise, the relation between θ and the upright draught T can be derived as listed in Table 1, where the floating equilibrium is found dependent on the aspect ratio (D/W) and upright draught T. The critical draughts T_1, T_2 and T_3 are formulated as follows:

$$T_1 = \frac{3D-\sqrt{9D^2-6W^2}}{6};$$
$$T_2 = \frac{3D-\sqrt{9D^2-8W^2}}{8};$$
$$T_3 = \frac{3D+\sqrt{9D^2-8W^2}}{8} \quad (9)$$

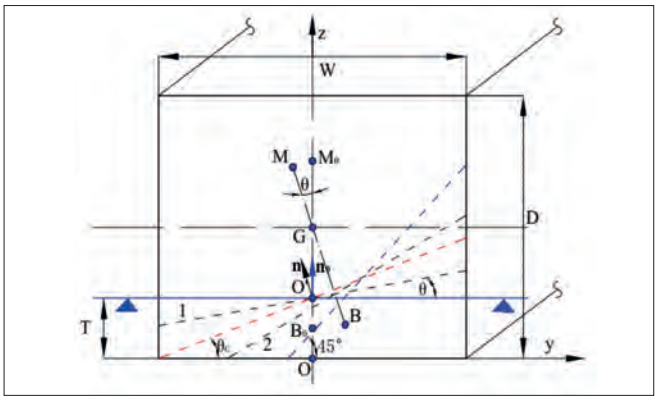

Fig. 3. Illustration of a floating prism with arbitrary rectangular section: the dashed lines refer to varied floating states (in anti-clockwise order, state 1→critical state θ_c→state 2→$\pi/4$)

Tab. 1. The floating equilibria for prism with arbitrary rectangular section

D/W	T	Floating equilibrium
$(0, \sqrt{6}/3)$	$(0, D/2]$	$\Theta = 0$
$[\sqrt{6}/3, \sqrt{8}/3]$	$(0, T_1)$	$\Theta = 0$
	$[T_1, D/2]$	$\theta = \tan^{-1}\left(\sqrt{\frac{12D(D-T)-2W^2}{W^2}}\right)$
$[\sqrt{8}/3, 1]$	$(0, T_1)$	$\Theta = 0$
	$[T_1, T_2]$	$\theta = \tan^{-1}\left(\sqrt{\frac{12D(D-T)-2W^2}{W^2}}\right)$
	(T_2, T_3)	$T = \frac{9\tan\theta(D\tan\theta - W^2)^2}{8W(\tan^2\theta - 1)^2}$
	$[T_3, D/2]$	$\theta = \tan^{-1}\left(\sqrt{\frac{12D(D-T)-2W^2}{W^2}}\right)$

Analogously, the floating equilibria can be derived in terms of the sectional aspect ratio, assuming the symmetry of the floating state. Furthermore, the equilibrium curves of a prism with varied aspect ratios (D/W) can be derived where the inflection points (the non-zero inflection points) can be observed distributed along lines as shown in Fig. 4. According to Fig. 4(a), a non-zero floating angle exists when the aspect ratio D/W is approximately larger than 0.82, which implies that asymmetrical floating states tend to occur at relatively large values of D/W. Otherwise, the prism would float symmetrically at any draught. That's why in most circumstances, only symmetric floating states are observed. Interestingly, the equilibrium curve is smooth when the sectional aspect ratio is less than around 0.96. Under this circumstance, the angle of inclination is less than the critical angle which could yield an inflection point. Note that there are two non-zero inflection points for each curve in the domain $\lambda \in [0, 0.5]$. Specifically, one inflection point approaches to around 25° and the other one approaches 45° with an increase of D/W. As shown in Fig. 4(b), the distribution of inflection points can be regressed into a linear function ($\theta = 73.1\,\lambda + 8.2$), except for the singular inflection point of $D/W = 1$.

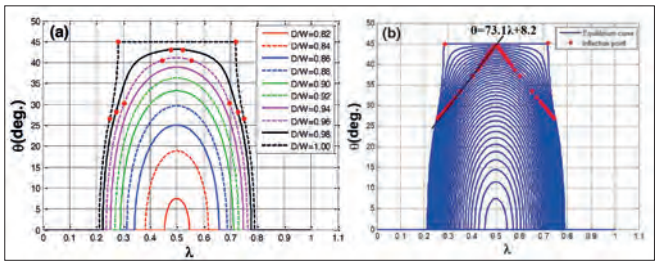

Fig. 4. The distribution of equilibrium curves and corresponding inflection points: (a) equilibrium curves for different sectional aspect ratios; (b) the distribution of inflection points and regressed function.

PARABOLIC CYLINDER

To illustrate the potential applications in naval and ocean engineering, the study of equilibrium is further extended to floating parabolic cylinders. As shown in Fig. 5, the parabolic profile curve can be assumed as the cross-section of a ship. To present the approach in a simplified manner, the cylinder is assumed uniform and then the centre of gravity $G(0, T(3D^2-5L^2)/5DL^2)$ can be derived, where T, D and L refer to the draught, breadth and the width of the flotation plane in the upright state, respectively.

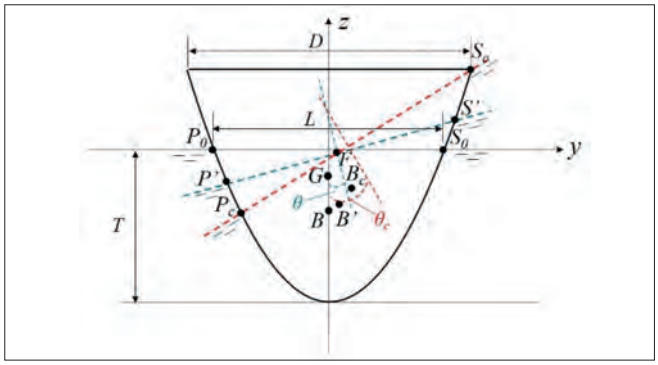

Fig. 5. Schematic section of a floating parabolic cylinder.

To generalize the derivation, the parabolic profile is written in a non-dimensional formula:

$$Z = KY^2 - N \quad (10)$$

where $Z = z/D$ and $Y = y/D$. The parameters K and N can be formulated as follows:

$$K = \frac{4TD}{L^2}$$
$$N = \frac{T}{D} \quad (11)$$

Further, the area of the immersed section can be derived as $A = 2TL/3D^2$. As illustrated in Fig. 5, assuming the cylinder

floats stably at an angle of inclination θ, the buoyancy centre translates from B to B' and the floatation line P_0S_0 becomes $P'S'$. For each specified floating cylinder, the maximum inclination angle θ_c is defined as the topside of the cylinder's contact with the water, yielding the corresponding flotation line P_cS_c. According to the conservation of the displaced volume and equation (10), the abscissas of the endpoints (P' and S') at inclination angle θ can be formulated as follows:

$$Y_{P'} = -\frac{L}{2D} + \frac{L^2}{8TD}\tan\theta \tag{12}$$

$$Y_{S'} = \frac{L}{2D} + \frac{L^2}{8TD}\tan\theta \tag{13}$$

In addition, θ_c can be obtained when $Y = ½$:

$$\theta_c = \tan^{-1}\left(\frac{4T(D+L)}{L^2}\right) \tag{14}$$

Therefore, the coordinate of the buoyancy centre can be obtained by calculating the double integral over the immersed section[13], taking into consideration the conservation of the area A of the immersed section. The coordinate of the buoyancy centre B can be formulated as follows:

$$Y_{B'} = Y_F + \frac{D^2}{A}\left[\frac{1}{12}L_\theta^3\sin\theta\cos^2\theta + \int_{Y_{P'}}^{Y_{S'}}(Y_F - Y)Z\,dY\right] \tag{15}$$

$$Z_{B'} = Z_F + \frac{D^2}{A}\left[\frac{1}{2}L_\theta\left(\frac{1}{12}L_\theta^2\sin^2\theta - Z_F^2\right)\cos\theta + \int_{Y_{P'}}^{Y_{S'}}\left(Z_F Z - \frac{1}{2}Z^2\right)dY\right] \tag{16}$$

where $L_\theta = (Y_{S'} - Y_{P'})$is to the length of the flotation line at an inclination angle of θ. Point F refers to the flotation centre, which is located at the centre of the line $P'S'$ Therefore, the coordinates of F are

$$Y_F = \frac{L^2}{8TD}\tan\theta \tag{17}$$

$$Z_F = \frac{L^2}{16TD}\tan^2\theta \tag{18}$$

Substituting equations (10), (12), (13), (17) and (18) into equations (15) and (16), the coordinate of B' can be derived as follows:

$$Y_{B'} = \frac{L^2}{8TD}\tan\theta \tag{19}$$

$$Z_{B'} = -\frac{2T}{5D} + \frac{L^2}{16TD}\tan^2\theta \tag{20}$$

Note that the abscissas of B' and F are identical[2]. According to Bouguer's theorem[16], the distance between B' and the metacentre M can be expressed as follows:

$$d_{B'}^M = \frac{I}{V} \tag{21}$$

where I and V refer to the moment of inertia of the plane of flotation and the immersed volume, respectively. Taking into consideration the homogeneity of the cylinder in the longitudinal direction, equation (19) can be simplified to

$$d_{B'}^M = \frac{R}{A} \tag{22}$$

where R denotes the moment of inertia of the flotation line with respect to F, which can be calculated as follows:

$$R = \int_{-\frac{1}{2}L_\theta}^{\frac{1}{2}L_\theta} s^2 ds = \frac{1}{12}L_\theta^3 \tag{23}$$

where L_θ is the flotation line at an inclination angle of θ, which can be written as $(Y_{S'} - Y_{P'})/\cos\theta$. Substituting equations (19), (20) and (23) into equation (22), the coordinates of M can be derived:

$$Y_M = \frac{L^2}{8TD}\tan^3\theta \tag{24}$$

$$Z_M = -\frac{2T}{5D} + \frac{L^2}{16TD}\left(\frac{3}{cos^2\theta} - 1\right) \tag{25}$$

To investigate the characteristics of the equilibrium curve practically, we confine the parameter $K \in [2, 3]$. Similarly, we use the relative density λ as the variant; it can be obtained as follows:

$$\lambda = \frac{\rho}{\rho_\omega} = \frac{L^3}{D(D^2 - L^2)} \tag{26}$$

According to equation (26), we can obtain the relation between the normalized draught and flotation line $T/D = KL^2/4D^2$. The equilibrium can be calculated by the conditions of force balance and stability as described before. Furthermore, the equilibrium curve can be derived along with $L/D \in (0, 1]$. Fig. 6(a) shows the profiles of a series of parabolic cylinders in the range $K \in [2, 3]$. The corresponding stable equilibrium curves are given in Fig. 6(b), where one can recognize the continuity of the equilibrium curves, located between approximately 60 degrees to 70 degrees. Also, the angle of inclination is increasing with an increase in the topological parameter K. Exploring a broader range of K, the equilibrium curve is found to be discontinuous (inflection points exist) for K around 1 (as shown in Fig. 7). Fig. 8 shows more profiles and their corresponding equilibrium curves around $K = 1$, through which the inflection point is found to be in the range $K \in [0.9, 1.7]$. Taking the parabolic cylinder as a vessel, we can conclude that the draught span for stable upright flotation is wider when the block coefficient becomes larger. As shown in Fig. 8(c), the distribution of the inflection points can be further formulated as

$$\theta = -1.71\ln(\lambda) + 55.684 \tag{27}$$

where $\lambda \in (0, 1]$. The above formulation can be applied to estimate the angle of inclination for a specified draught when a discontinuity exists in the equilibrium curve. Those inflection points should be noted during the operation of the ship to avoid a severe variation of the floating state.

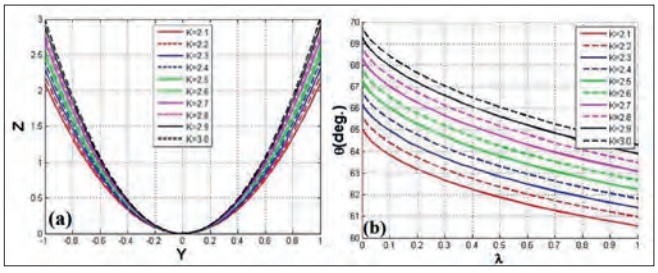

Fig. 6. Profiles of a series of parabolic cylinders (a) and their corresponding equilibrium curves (b) for K∈[2, 3].

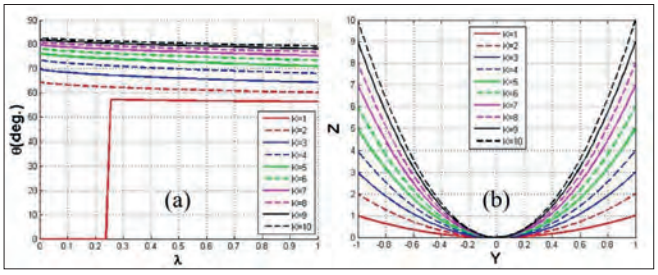

Fig. 7. The distribution of equilibrium curves (a) and corresponding profiles (b) for K∈[1, 10].

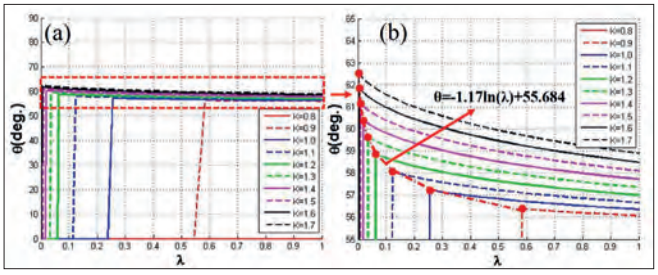

Fig. 8. A series of equilibrium curves (a) for K∈[[0.8, 1.7], where the distribution of the inflection points (labeled by rectangles in (a)) is regressed (b).

EXPERIMENTAL VERIFICATION

To verify these theoretical results, an experiment was conducted in the flume of the laboratory LOC (Laboratório de Ondas e Correntes) of the Federal University of Rio de Janeiro. As shown in Fig. 9, a hollow square prism with 5×5 grid was designed to simulate a uniform prism whose weight can be adjusted by filling the grids symmetrically with ballast. In these tests, uniform iron bars with different diameters were applied as ballast: their lengths are identical to that of the prism. Waterproof foam lids were used on both ends. The minimum relative density of the prism (i.e., a hollow prism) was 0.06 and the maximum about 0.87, as listed in Table 2. For each round of testing, the prism was released from an upright state and the inclination angle measured after the reaching of a stable floating state. As shown in Fig. 10, various floating states can be observed, including several asymmetrical ones.

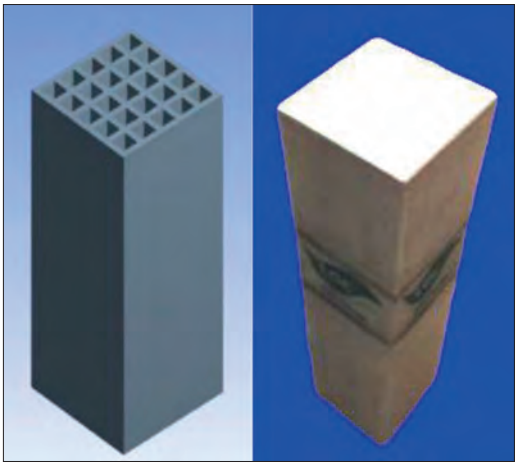

Fig 9. The hollow model with 5×5 grid structure (left) and the practical prism model with lids prepared for testing (right).

Tab. 2. The test matrix and stable floating angle.

Case	Relative density	Stable angle(°)	Case	Relative density	Stable angle(°)
1	0.06	0	10	0.46	45
2	0.20	13	11	0.51	45
3	0.23	24	12	0.56	45
4	0.26	28	13	0.61	45
5	0.29	31	14	0.67	44
6	0.32	44	15	0.72	42
7	0.36	44	16	0.76	27
8	0.39	45	17	0.81	14
9	0.42	45	18	0.87	1

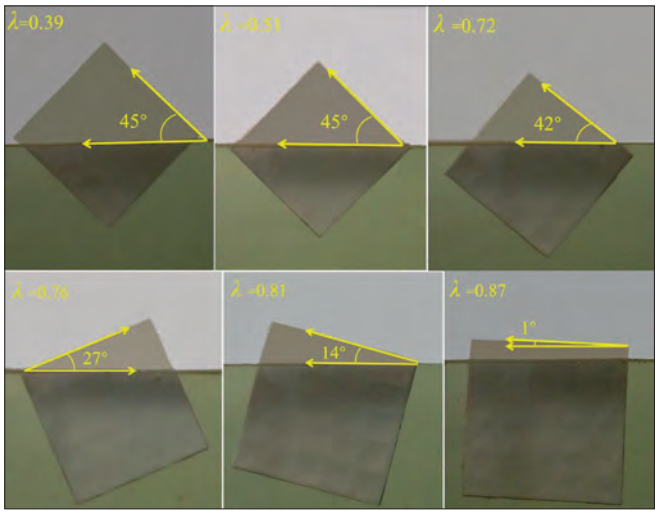

Fig. 10. The typical floating states corresponding to the cases in Table 2.

As shown in Fig. 11, the experimental results have been compared with the analytical results and the results of [1]. Overall, the present analytical results agree better with the experimental results than do those of [1]. It can be noted that the scatter of the experimental results deviates slightly from the analytical results near the inflection points. This is because the floating state becomes quite sensitive to the relative density near those inflection points. The experimental uncertainty should also be responsible for the deviation, due to the machining and assembly error of the square prism. Further, the symmetry of the floating equilibrium curve is also verified by the experimental results, with respect to the centerline at $\rho/\rho_w = 0.5$. It is worth noting that the inflection points revealed in the present work make the equilibrium curve possess a significant 'plateau' and narrow transition range from $\theta = 0°$ to 45°. According to the present floating equilibrium curve, one should note that the magnitude of draught of floating body could affect the stable floating state significantly, which, for many floating structures, must be strictly supervised to avoid operational risks. For example, the relative density of a fully loaded cubic barge is usually larger than 0.8, thus its normal stable floating angle is zero. However, improper loading could make the relative density collapse to 0.2~0.8. Therefore, an initial inclination of the vessel

may occur which could lead to capsizing. In conclusion, the equilibrium curve should be considered by the designer and operator of floating structures whose relative density or weight could be varied frequently, in addition to the use the equilibrium curves to adjust the floating state actively.

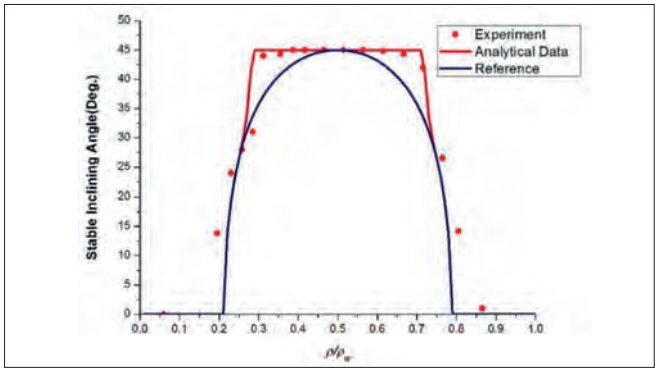

Fig. 11. Comparison of analytical and experimental results

CONCLUSIONS

In the present article, the phenomenon that symmetric geometries can float asymmetrically has been studied analytically and experimentally. The intact floating equilibrium curve for a prism and a parabolic cylinder have been derived in detail, finding several characteristics which are revealed as different from those found in the literature. The characteristics of the inflection points in the equilibrium curve have been analysed, providing an improved interpretation of them in physical terms. Generalizing these results, the analysis of floating equilibria has been extended to prisms with arbitrary rectangular section. Some interesting features are revealed concerning the distribution of the equilibrium curves corresponding to a series of sectional aspect ratios. To illustrate the case of a vessel, the floating equilibrium of a parabolic cylinder was further investigated. The characteristics of its equilibrium curves have been obtained analytically, which could be meaningful to the design of floating structures in naval and ocean engineering.

Moreover, to verify the floating equilibrium curve, experiments were conducted with a uniform square prism with adjustable relative density. According to the experimental results, good agreement is reached relative to the presented analytical results. In terms of the applications of equilibrium curves, the behaviour of the floating equilibrium should be understood and could be taken advantage of to avoid a damaging event of floating structures and enhance the efficiency of operation, especially for those floating vessels with a frequent variation of loading. The present study illustrates an approach to comprehend the floating equilibrium through several fundamental geometries, which can be extended to the investigation of the floating equilibrium of more complex geometries in future work. Besides, the two-dimensional floating state should also be considered in the future, namely considering both transversal and longitudinal inclination simultaneously, which will be more practical for applications.

ACKNOWLEDGMENT

The study is financed in part by the CNPq (Conselho Nacional de Pesquisa-Brazilian National Research Council), the National Natural Science Foundation of China (52201304 and 52271336), which are gratefully acknowledged. The colleagues from LOC have contributed with efforts and ideas, which are gratefully appreciated.

REFERENCES

1. E. N. Gilbert, "How things float," *Journal American Mathematical Monthly*, vol. 3, pp. 201 216, 1991.
2. J. Mégel and J. Kliava, "Metacenter and ship stability," *American Journal, American Association of Physics Teachers*, vol. 78, no. 7, pp. 738 747, 2010.
3. A. Karczewski, "The Influence of The Cuboid Float's Parameters on The stability of A Floating Building," *Polish Maritime Research*, vol. 27, no. 107, pp. 16 21, 2020.
4. J. Li, "Analysis of The Dynamic Response of Offshore Floating Wind Power Platforms in Waves," *Polish Maritime Research*, vol. 27, no. 108, pp. 17 25, 2020.
5. K. J. Spyrou, "The stability of floating regular solids," *Ocean Engineering*, vol. 257, no. 111615, 2022.
6. D. G. AS, RULERS FOR CLASSIFICATION: Inland Navigation vessels, part 6 Additional class notations, 2015.
7. H. Auerbach, "Sur un problem de M. Ulam concernant l'équilibre des corps flottants (On a problem of Mr. Ulam concerning the equilibrium of floating bodies)," *Studia Math*, vol. 7, pp. 121 142, 1938.
8. C. L. Bernard, Stability and equilibrium of floating bodies, London: Constable and Company Limited, 1914.
9. V. Bertram, Practical ship hydrodynamics, 2nd ed., Oxford: Elsevier Butterworth Heinemann, 2012.
10. A. Biran, Ship hydrostatics and stability, 1st ed., Oxford: Elsevier Butterworth Heinemann, 2003.
11. S. N. Blagoveshchensky, Theory of ship motions (Transl. from the 1st Russian edition), New York: Dover Publications, 1962.
12. H. E. Rossell and L. B. Chapman, Principles of Naval Architecture, Vol. 1, New York: Soc. Naval Architecture and Marine Engineering, 1941.
13. E. H. Lockwood, A book of curves, Cambridge University Press, 2007.

14. S. M. Ulam, "A collection of mathematical problems," *Science*, vol. 132, pp. 665 666, 1960.

15. L. Montejano, "On a problem of Ulam concerning a characterization of the sphere," *Studies in Applied Mathematics*, vol. 3, pp. 243 248, 1973.

16. P. Bouguer, Traité du Navire, de sa construction, et de ses mouvemens (Tratise on Ship's Construction and Movements), Paris: Jombert, 1746.

17. K. D'Angremond and F. C. Van Roode, Breakwaters and Closure Dams, London: Spon Press, 2004.

18. P. Erdös, G. Schibler and R. C. Herndon, "Floating equilibrium of symmetrical objects and the breaking of symmetry, Part 1: Prisms," *Am. J. Phys.*, Am. J. Phys., vol. 60, no. 4, pp. 335-345, 1992.

19. H. Ghassemi, I. Ghamari and A. Ashrafi, "Numerical Prediction of Wave Patterns Due to Motion of 3D Bodies by Kelvin-Havelock Sources," *Polish Maritime Research*, vol. 23, no. 92, pp. 46-58, 2016.

20. T. L. Heath, The works of Archimedes, Dover Publications, 2005.

21. K. J. Rawson and E. C. Tupper, Basic Ship Theory, 5th ed., London: Longman, 2001.

22. D. R. Derrett and C. B. Barras, Ship stability for masters and mates, 6th ed., Oxford: Elsevier Butterworth-Heinemann, 2006.